UC San Diego

UC San Diego Previously Published Works

Title

Scaling Parameters for Dynamic Diffusion-Reaction over Porous Catalysts

Permalink

https://escholarship.org/uc/item/9bc7v3kv

Journal

Industrial & Engineering Chemistry Research, 54(16)

ISSN

0888-5885

Author

Herz, Richard K

Publication Date

2015-04-29

DOI

10.1021/ie503860w

Peer reviewed

eScholarship.org Powered by the California Digital Library
University of California

Scaling parameters for dynamic diffusion-reaction over porous catalysts

Richard K. Herz*

NanoEngineering Department, Jacobs School of Engineering, University of California, San Diego, CA, USA 92093-0448

E-mail: rherz@ucsd.edu

Cite as: Herz, R.K., Ind. Eng. Chem. Res., **2015**, 54 (16), pp 4095-4102. doi: 10.1021/ie503860w

Abstract

The effect of diffusion resistance in porous solid catalysts on reaction rate during periodic cycling of CO concentration is shown for CO oxidation over Pt/Al_2O_3 by numerical simulation. At some cycling frequencies, the average reaction rate during cycling is higher than the steady-state rate at the mean CO concentration, as expected for this nonlinear, reactant-inhibited reaction. In order to identify major aspects of dynamic diffusion-reaction behavior, a simple kinetic mechanism that shows the main features of CO oxidation and other reactions with significant inhibition by reactants is investigated. A single dimensionless parameter group, the dynamic diffusion coefficient, is added when going from steady-state to unsteady-state diffusion-reaction equations. In the dynamic diffusion coefficient, the rate at which gas-phase reactant diffuses is reduced by the surface adsorption capacity of the catalyst. The frequency at which the peak average rate occurs is controlled by the dynamic diffusion coefficient. **Keywords**: dynamic, diffusion-reaction, reaction-diffusion, heterogeneous catalyst, porous catalyst, periodic operation, unsteady state.

*To whom correspondence should be addressed

Introduction

Scott Fogler's textbooks[1,2] helped teach my students the subject of reaction engineering for over 20 years at UC San Diego. Scott was kind enough to include my Reactor Lab software[3] with the later editions of his reaction engineering texts.

I had the pleasure to meet Scott many years ago in Michigan, when I worked at GM Research Labs. People from U. Michigan, Wayne State, GM, Ford, Dow and other research labs in the area got together frequently at meetings of the Michigan Catalysis Society, where we socialized and listened to visiting speakers.

At one of those meetings, Joe Kummer of Ford asked me about the research I was doing. I explained something about diffusion plus elementary step reaction models (microkinetics). Joe replied, "steady state is boring!" Taken aback, I later realized that he had a point and decided to focus on catalysis under dynamic conditions.[4] The microkinetic models of Herz and Marin[5] were extended to dynamic conditions by our colleague at GM, Byong Cho, who predicted interesting space-time patterns of components in porous catalysts.[6] We developed microkinetic diffusion-reaction models, which we fit to time-resolved experimental measurements of CO oxidation.[7-10]

Peter Silveston would sometimes visit the Michigan Catalysis Society from nearby Waterloo University in Ontario, Canada. Peter later edited the book *Composition Modulation of Catalytic Reactors*.[11] Whereas we usually teach students to design systems to operate at the optimal steady state, works in this book demonstrated that periodic operation of reactors can sometimes achieve higher conversion of reactants than steady-state operation. Peter, along with Robert Hudgins, recently published a related book, *Periodic Operation of Reactors*,[12] which reviews additional modes of operation such as temperature cycling.

The result that dynamic operation of a reactor has the potential to achieve better performance than steady-state operation is both an intriguing and potentially profitable idea.[13,14] In order for a reaction system to have the possibility of rate enhancement during composition modulation, the kinetics must be nonlinear.[13,15-18]

Models with equations that describe dynamic diffusion and reaction in porous catalysts during composition forcing have been developed for specific reactions to explain experimental measurements. Many of these works have studied CO oxidation [6-10,19] or three-way automotive catalytic reactions[20] with rather complex models.

There is a need for studying periodic operation with more general models that exhibit the main features of experimental results but whose diffusion-reaction equations are simple such that parameters that determine performance can be identified. An important feature for any useful model is description of the maximum capacity of a porous catalyst for adsorbed components. Work with models that specify linear adsorption and no limit on surface coverage[21] effectively add only a reversible step to a homogenenous reaction system.

In this work, results for reactant composition cycling of CO oxidation in a porous catalyst are presented. Significant aspects of the steady-state and dynamic behavior seen for CO oxidation, such as rate enhancement during composition cycling, can also be obtained with a simple reaction model with reactant inhibition. Diffusion-reaction equations are developed for the simple model. Dimensionless scaling parameters are identified that explain the frequency range in which maximum rate enhancement is obtained under limiting conditions.

Even with a simple reaction model under limiting conditions, the parameter and operating condition ranges are large and outside the scope of this work. Thus, the goal of this work is to stimulate further study of the dynamic operation of diffusion-reaction systems.

Periodic Operation of a CO Oxidation Catalyst

Fig. 1 shows plots of predicted average rate *vs.* frequency for periodic operation of a CO oxidation catalyst. CO was cycled in a sine wave while the O_2 pressure was held constant. The detailed diffusion-reaction model solved was that of Nett-Carrington and Herz[9] for a porous Pt/Al_2O_3 catalyst. The model was developed from experiments in which gas concentrations were measured (a) for gas flowing over a porous catalyst layer and (b) at the equivalent center of the layer where a no-flux boundary condition was closely approached.[8] Isothermal conditions were assumed and were closely approached in the experiments used to

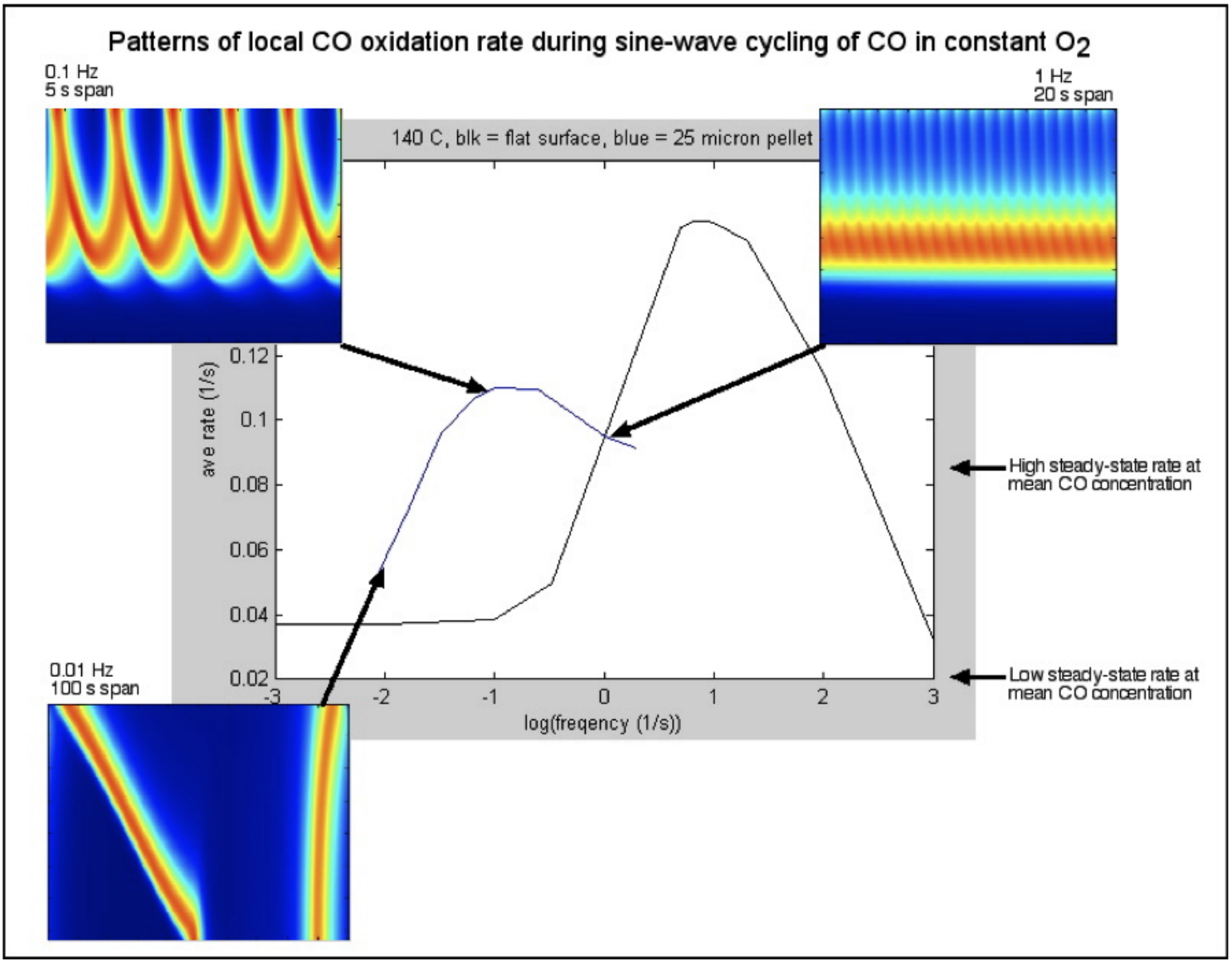

Fig. 1. Predicted patterns of local CO oxidation rate during sine-wave cycling of CO in constant O_2 over Pt/Al_2O_3. Curves are average overall rate during cycling vs. $\log_{10}$ of frequency. Black (peak on right) = hypothetical "flat" surface with no diffusion resistance. Blue (peak on left) = rate over 25 micron porous catalyst layer. Color insets are space-time patterns of local reaction rate in the porous layer. The model of Nett-Carrington and Herz[9] and the parameter values in Table 1 of that work apply for the porous layer, except that $\phi_1 = 0.20$ (fraction site-type 1) and $C^{surf}{}_{tot}$= 44 mol of total surface sites per m^3 layer. T = 140 °C, 0-16 Pa-CO, 110 Pa-O_2. Rate shown is turnover frequency (product molecules formed per site per second).

develop the model.[8,9]

The stiff system of partial differential equations for the elementary-step model and porous catalyst were integrated numerically using the Crank-Nicolson method[9,22] with 40 equally spaced nodes. An empty-surface initial condition was specified, and the system of equations was integrated until a steady cycling pattern developed. Average rates are the mean of local reaction rates within the layer during one period. Computation time is long for low frequencies but a steady cycling pattern is reached after only a few cycles.

The curve that peaks on the right side of the figure is the average rate predicted for these kinetics over a hypothetical "flat" catalyst surface with no mass transfer resistance.

The curve that peaks on the left side of the figure is the average rate predicted over a 25 micron-thick porous catalyst layer at 140 °C, 0-16 Pa-CO, 110 Pa-O_2. Compared to the results for the flat catalyst, the peak in rate is lower in height and is at two-orders of magnitude slower frequency. Although the presence of diffusion resistance appears to degrade the performance of the catalyst, the "flat" case with no diffusion resistance is hypothetical and most industrial catalysts are porous for a variety of reasons.

The color insets show space-time patterns of local reaction rate within the porous layer. The vertical dimension is position in the layer and the horizontal dimension is time. The top of each color inset is at the outer boundary of the layer that is exposed to flowing gas. The bottom is the inner boundary of the layer with a no-flux boundary condition. Left-to-right is the progression of time. The local reaction rate is on a color scale (MATLAB jet) that is blue for low rate and red for high rate. There are no space-time patterns for the flat surface because there is no spatial variation in that case.

At low cycling frequency, CO penetrates to the inner boundary of the porous catalyst layer, and the rate is inhibited or "quenched" everywhere in the layer during part of the cycle. At intermediate frequency near the peak in rate, there is a periodic looping pattern of local rate in the layer. At high frequency, relaxed steady-state conditions are approached such that the average rate during cycling approaches the steady-state rate at the mean

concentration.

Fig. 2 shows predicted steady-state rate *vs.* CO pressure under steady-state conditions over the flat surface and porous layer under the same conditions as Fig. 1. Near the mean CO pressure, there is a region for the porous catalyst where there are two stable steady states possible at a given CO pressure. This rate multiplicity is caused by the coupling of the nonlinear, Langmuir-Hinshelwood, reactant-inhibited kinetics with diffusion resistance.[23] For these kinetics, there are no multiple steady states over the flat surface with specified external CO concentration. Other CO oxidation kinetics may admit to intrinsic rate multiplicity.[24,25] Note that the rate over the porous catalyst (diffusion resistance) is greater than the rate over the flat surface (no diffusion resistance) for external CO pressures greater than 2.2 Pa, CO/(16 Pa) > 0.14. The effectiveness factor is greater than one in this range for the CO-inhibited reaction. For a different case with either the flat or porous catalyst inside a CSTR, multiple steady states of reaction rate *vs.* reactor inlet CO concentration can occur due to coupling of the nonlinear kinetics with the material balance over the reactor.[26]

High reaction rate occurs when coverages of both adsorbed CO and adsorbed O over the surface are at intermediate values, since the rate determining step is reaction of adsorbed CO and O to form CO_2. The lower branch of the curve for the steady-state reaction in the porous layer is at conditions where the coverage of the catalyst surface by CO is high, the coverage of O is low, and the rate is relatively low.

At the maximum CO pressure during cycling, if steady-state were to be approached, the coverage of CO would be high and the rate would be low. This condition occurs at low cycling frequencies, as seen in the left-most space-time color inset in Fig 1. At intermediate and high frequencies, the layer never becomes covered with high CO everywhere, and high reaction rates are obtained at points within the layer.

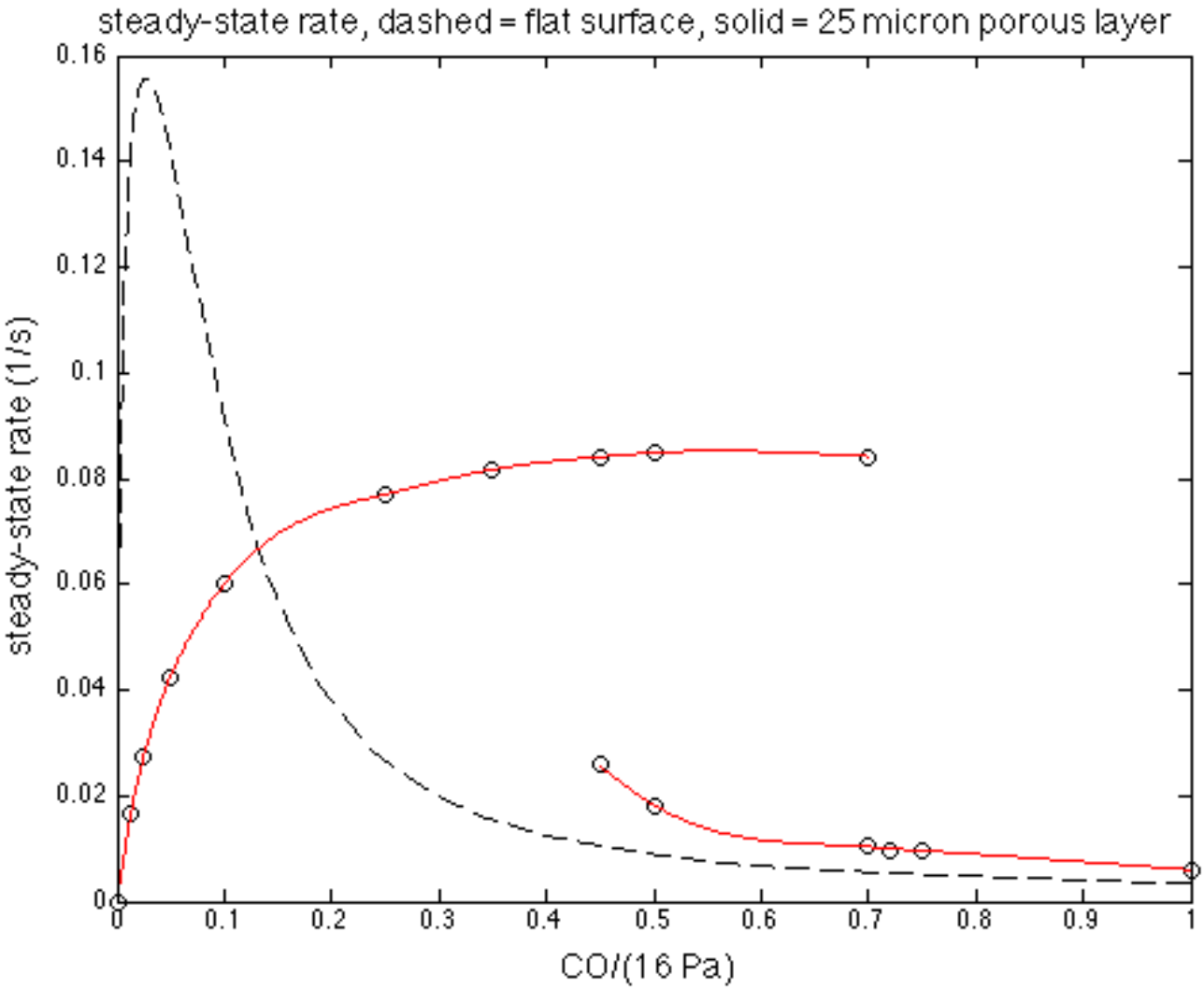

Fig. 2. Predicted steady-state CO oxidation rate vs. external CO pressure in constant O_2 over Pt/Al_2O_3. Dashed line = rate over hypothetical "flat" surface with no diffusion resistance. Double solid lines = rate over porous catalyst layer showing rate multiplicity. Same conditions as Fig. 1

The rate at the peaks of both curves in Fig. 1 during cycling are higher than the steady-state rate at the mean CO concentration on the high-rate branch of the curve in Fig. 2. That is, the reaction rate during cycling is higher than at steady-state at the mean concentration. In Fig. 1, note the arrow and label in the right margin that refers to the porous layer: "High steady-state rate at mean CO concentration."

The rate enhancement can be explained in terms of storage by the surface of adsorbed reactants in one half of a cycle and desorption and reaction of the stored reactants in the other half of the cycle, with CO and O_2 being stored in successive halves of the cycle.[6,27]

The magnitude and location of the mean rate *vs.* frequency curve for a porous catalyst will vary with many factors, including layer thickness, active site concentration, and shape of the composition forcing function.

Periodic Operation With Simplified Kinetics

The kinetic mechanism used for Figs. 1 and 2 are complex since they were developed to explain experimental measurements. A simple reaction mechanism, which exhibits the same main qualitative results, can be used to highlight the relationships between catalyst parameters and conditions and how they affect rate *vs.* frequency curves.

The reaction mechanism modeled in this work is:

1) A (g) + S $\rightleftharpoons$ AS

2) AS + S $\rightharpoonup$ P (g) + 2S

with overall stoichiometry A $\rightharpoonup$ P.

Step 1 is reversible adsorption of reactant component A over surface sites S. Step 2 is the rate determining step and is assumed to be far from equilibrium under the conditions considered. Assumptions of Langmuir-Hinshelwood kinetics apply such as random distribution of adsorbates over sites with constant properties.

At low concentrations of A, the overall rate is first-order in A. At intermediate concentrations of A, when the concentrations of AS and S are equal, the overall rate reaches a maximum. At high concentrations of A, the rate is low because the concentration of vacant

sites S is low, and the overall rate is negative-order in A. The main feature of this model, inhibition of the reaction by a reactant, is also a key feature of some industrially important reactions including CO oxidation.

In the limit of small surface rate constant and the absence of mass-transport resistance, the steady-state rate equation is:

$$-r_A = \frac{k_2 K_A C_A}{(1 + K_A C_A)^2} \tag{1}$$

where C_A is the gas-phase concentration of the reactant, K_A is the equilibrium adsorption constant for adsorption of A, and k_2 is the rate constant of step 2. This is the same form of rate equation used by Wei and Becker[23] to study the effects of diffusion resistance on CO oxidation over porous catalysts. A plot of steady-state rate *vs.* reactant concentration for this equation is qualitatively similar to the curve in Fig. 2 for the flat surface.

Other mechanisms with different step 2 reactions should also exhibit sufficient nonlinearity to provide rate enhancement during composition cycling. Examples include (a) AS + AS $\rightarrow$ P (g) + 2S and (b) A + AS $\rightarrow$ P (g) + S. These mechanisms will change from second-order in A to zero-order as the concentration of A increases. A mechanism with AS $\rightarrow$ P (g) + S will change from first-order to zero-order as the concentration of A increases, which is a regime that should not produce rate enhancement during cycling.[17]

The dimensionless equation for the dynamic system in a 1D porous catalyst layer is, for the adsorbed reactant at each position within the layer:

$$\frac{d\theta}{d\tau} = \kappa_{ads}\psi(1-\theta) - \theta - \kappa_{rxn}\theta(1-\theta) \tag{2}$$

with dimensionless variables and parameters:

$$\theta = \text{fractional coverage of surface by adsorbed reactant} \tag{3}$$

$$\tau = t(s)k_{-1}(s^{-1}) = \text{dimensionless time} \tag{4}$$

where k_{-1} is the reactant desorption rate constant in step 1,

$$\kappa_{ads} = \frac{k_1(\mathrm{m^3 mol^{-1} s^{-1}})C_{A,max}(\mathrm{mol\ m^{-3}})}{k_{-1}(\mathrm{s^{-1}})} = \text{reactant adsorption rate constant} \tag{5}$$

$$\psi = \frac{C_A}{C_{A,max}} = \text{gas-phase reactant concentration} \tag{6}$$

$$\kappa_{rxn} = \frac{k_2(\mathrm{s^{-1}})}{k_{-1}(\mathrm{s^{-1}})} = \text{reaction rate constant} \tag{7}$$

The dimensionless equation for the dynamic system in a 1D porous catalyst layer is, for the gas-phase reactant:

$$\frac{\partial \psi}{\partial \tau} = \left(\frac{\kappa_{diff}}{\epsilon}\right)\left(\frac{\partial^2 \psi}{\partial \lambda^2}\right) - \alpha\left[\kappa_{ads}\psi(1-\theta) - \theta\right] \tag{8}$$

with dimensionless parameters:

$$\kappa_{diff} = \left(\frac{D_e}{L^2}\right)\left(\frac{1}{k_{-1}}\right) = \text{dimensionless diffusion coefficient in layer of thickness } L \tag{9}$$

$$\epsilon = \text{void fraction in porous catalyst layer} \tag{10}$$

$$\lambda = \frac{z(\mathrm{m})}{L(\mathrm{m})} = \text{position within layer} \tag{11}$$

with z measured from the interior, zero-flux boundary,

$$\alpha = \frac{A(\mathrm{m^2})C_{A,max}^{\mathrm{surface}}(\mathrm{mol\ m^{-2}})}{\epsilon V(\mathrm{m^3})C_{A,max}^{\mathrm{gas}}(\mathrm{mol\ m^{-3}})} = \text{surface-to-gas capacity ratio} \tag{12}$$

where A is the active internal surface area of the layer, and V is the volume of the layer. The surface-to-gas capacity ratio α is the ratio between the maximum number of moles that can be adsorbed on the surface in the layer to the maximum number of moles of gas that can be held in the pore volume of the layer.[9,7] The boundary conditions for the gas-phase

equation are:

$$\psi(\lambda = 1, t) = \psi_1(t) \tag{13}$$

$$\left[\frac{d\psi}{dt}\right]_{\lambda=0} = 0 \tag{14}$$

For specified parameter values and initial conditions, the system behavior can be computed for specified reactant concentration forcing functions $\psi_1(t)$ over the external boundary of the layer. Hsiao[28] has written a general diffusion-reaction solver that can solve this problem as well as problems with arbitrary kinetic schemes.

Even with such simple kinetics, there are four dimensionless parameters to specify (κ_{ads}, κ_{rxn}, (κ_{diff}/ϵ), α) and two differential equations to integrate (surface, gas) in order to solve the dimensionless system.

The system can be simplified by considering a limiting case that will hold over many practical catalyst systems, including catalytic CO oxidation. This simplification will allow identification of scaling parameters and explanation of the frequency range at which maximum rate enhancement occurs. The limiting case is obtained when the surface reaction is rate limiting and the surface capacity for adsorbed reactant is large.

First, specify that the surface reaction rate constant is small, $\kappa_{rxn} << 1$, such that step 1 in the mechanism is in close approach to equilibrium adsorption of reactant. The equation for reactant gas in the catalyst pores becomes:

$$\frac{\partial\psi}{\partial\tau} = \left(\frac{\kappa_{diff}}{\epsilon\alpha}\right)\left[\frac{1}{\frac{1}{\alpha} + \frac{\kappa_{ads}}{(1+\kappa_{ads}\psi)^2}}\right]\left[\frac{\partial^2\psi}{\partial\lambda^2} - \phi^2\frac{\psi}{(1+\kappa_{ads}\psi)^2}\right] \tag{15}$$

where the Thiele modulus ϕ is given by:

$$\phi^2 = \left(\frac{\kappa_{rxn}\kappa_{ads}}{\kappa_{diff}/(\epsilon\alpha)}\right) = \frac{L^2}{D_e}\left[k_2(A/V)\kappa_{ads}C_{A,max}^{\text{surface}}\right] = \frac{L^2(\text{m}^2)}{D_e(\text{m}^2\ \text{s}^{-1})}\left[K_r(\text{s}^{-1})\right] \tag{16}$$

This Thiele modulus is equivalent to that defined for these kinetics by Wei and Becker.[23]

Since reactant surface coverages closely approach equilibrium under this specification,

only the gas-phase equation must be solved under dynamic conditions: the equilibrium surface coverage at each time and position can be computed from the gas concentration. This is also termed a quasi-steady-state approximation for adsorbed components.[21]

Next, specify that the surface-to-gas capacity ratio is large, $\alpha >> 1$. This is a reasonable condition for many systems, including the system shown in Fig. 1. For example, $\alpha = 100$ for 0.1% CO in 1 atm-gas at 360 K over 2% exposed, 1 wt% Pt on 1 g/cm^3 alumina with $\epsilon = 0.3$.

The equation for reactant gas in the catalyst pores becomes:

$$\frac{\partial \psi}{\partial \tau} = \left(\frac{\kappa_{diff}}{\epsilon \alpha}\right) \left[\frac{(1+\kappa_{ads}\psi)^2}{\kappa_{ads}}\right] \left[\frac{\partial^2 \psi}{\partial \lambda^2} - \phi^2 \frac{\psi}{(1+\kappa_{ads}\psi)^2}\right] \tag{17}$$

For this limiting case, the number of differential equations has been reduced from two to one, and the number of dimensionless parameters has been reduced from four to three: κ_{rxn}, κ_{ads}, and $(\kappa_{diff}/(\epsilon\alpha))$. The Thiele modulus ϕ is a combination of the other dimensionless parameters:

$$\phi^2 = \left(\frac{\kappa_{rxn}\kappa_{ads}}{\kappa_{diff}/(\epsilon\alpha)}\right) \tag{18}$$

$$\phi^2 = (\epsilon\alpha)\left(\frac{L^2}{D_e}\right)(\kappa_{rxn}\kappa_{ads}k_{-1}) \tag{19}$$

Under steady-state conditions:

$$\frac{\partial^2 \psi}{\partial \lambda^2} = \phi^2 \frac{\psi}{(1+\kappa_{ads}\psi)^2} \tag{20}$$

where the two boundary conditions are the same as above, Eqns. 13 and 14, for the dynamic gas-phase equation. The dimensionless steady-state solution is determined by two values: those of ϕ and κ_{ads}. Solutions of this steady-state equation were presented by Wei and Becker.[23] Plots of steady-state rate *vs.* reactant concentration will look similar to the curves for the porous catalyst in Fig. 2, also showing the possibility of multiple steady states in the presence of diffusion resistance.

Finally, redefine the dimensionless time:

$$\frac{\partial \psi}{\partial T} = \left[\frac{(1+\kappa_{ads}\psi)^2}{\kappa_{ads}}\right]\left[\frac{\partial^2 \psi}{\partial \lambda^2} - \phi^2 \frac{\psi}{(1+\kappa_{ads}\psi)^2}\right] \tag{21}$$

$$T = \left(\frac{\kappa_{diff}}{\epsilon\alpha}\right)\tau \tag{22}$$

$$t(\mathrm{s}) = (\epsilon\alpha)\left(\frac{L^2}{D_e}\right)T \tag{23}$$

The differential equation for the limiting case, Eqn. 21, was solved with an explicit finite-difference numerical method with 40 equally spaced nodes. An empty-surface initial condition was specified, and the system of equations was integrated until a steady cycling pattern developed. Average rates are the mean of local reaction rates within the layer during one period.

The gas phase concentration of reactant over the outer boundary of the layer ψ_1 was changed in steps and was also cycled in square waves and sine waves in different numerical experiments. During periodic operation, the real-time frequency ω (s^{-1}) can be defined by its use in a sine-wave forcing function:

$$\psi_1(t) = 0.5\,[1 + \sin(2\pi\omega t)] \tag{24}$$

The dimensionless frequency Ω can be defined by:

$$\psi_1(T) = 0.5\,[1 + \sin(2\pi\Omega T)] \tag{25}$$

$$\Omega = (\epsilon\alpha)\left(\frac{L^2}{D_e}\right)\omega \tag{26}$$

Scaling Parameters

In going from the steady-state system (Eqn. 20) to the dynamic system, (Eqn. 17), only one more dimensionless parameter is added: $(\kappa_{diff}/(\epsilon\alpha))$. This parameter can be considered a dynamic diffusion coefficient in which the surface-to-gas capacity ratio α modifies the diffusion dynamics. For example, a larger surface capacity slows the rate of penetration of reactant gas into the porous catalyst layer.

The system has been simplified sufficiently such that we can see some interesting scaling cases.

<u>*Case 1*</u>: Change any two or more components of the dynamic diffusion coefficient $(\kappa_{diff}/(\epsilon\alpha))$ $= (\epsilon\alpha L^2/D_e)$ such that the value of the group remains constant.

Result 1: The steady-state solution of dimensionless concentration profile $\psi(\lambda)$ remains unchanged because the Thiele modulus ϕ and the adsorption constant κ_{ads} remain unchanged.

Result 2: The dynamic solutions of dimensionless concentration profiles remain unchanged in both dimensionless time $\psi(\lambda, T)$ and real time $\psi(\lambda,t)$ as the external reactant concentration is varied. This result is true for arbitrary forcing functions.

Result 3: Although the dimensionless solutions remain unchanged, the dimensioned rate of reaction over the catalyst layer (mol/s) will change if the ratio L^2/D_e changes.

<u>*Case 2*</u>: Change κ_{diff} and κ_{rxn} by the same factor such that the Thiele modulus ϕ remains constant but the dynamic diffusion coefficient value changes. Keep κ_{ads} constant.

Result 1: The steady-state solution $\psi(\lambda)$ remains unchanged.

Result 2: The dynamic solution in dimensionless time $\psi(\lambda, T)$ remains unchanged.

Result 3: The dynamic solution in real time $\psi(\lambda,t)$ changes because the dynamic diffusion coefficient, which relates t(s) and T, has changed.

The results of Case 2 prove an imperative for kinetic studies: Dynamic experiments should be performed in addition to steady-state experiments, since two catalytic systems can exhibit the same steady-state behavior but different dynamic behavior.[29]

Frequency at Maximum Rate Enhancement

The solutions for the simplified kinetic model during periodic operation show peaks in average rate *vs.* frequency, similar to those seen in Fig. 1 for a detailed kinetic model of CO oxidation. The results for the simplified model are shown in Fig. 3. The color insets show space-time patterns of local reaction rate within the porous layer, as described above for Fig. 1. Also shown is the local reaction rate pattern for steady state at the mean reactant concentration over the layer.

The simplified kinetics allow us to understand some of the features of the average rate *vs.* cycling frequency curves. Case 1, Result 2 above shows that systems with constant ϕ, κ_{ads} and $(\epsilon\alpha L^2/D_e)$ will exhibit the same dimensionless solutions during periodic operation on rate *vs.* ω (s^{-1}) real-time frequency plots.

Case 2, Result 3 shows that systems with constant ϕ and κ_{ads} but <u>different</u> $(\epsilon\alpha L^2/D_e)$ will exhibit <u>different</u> curves on rate *vs.* ω (s^{-1}) plots. The frequency at which the peak in rate occurs is related to the surface-to-gas capacity ratio α as well as the layer thickness and effective diffusivity.

Case 2, Result 2 shows that systems with constant ϕ and κ_{ads} but <u>different</u> $(\epsilon\alpha L^2/D_e)$ will fall on the <u>same</u> curve on rate *vs.* Ω dimensionless frequency plots.

For $\kappa_{ads} = 100$ and $\phi = 34$, rate multiplicities exist at the mean concentration on the steady-state rate *vs.* concentration plot. Steady-state profiles were presented by Wei and Becker[23] for these parameter values.

For these parameter values, the peak in average rate during cycling occurs at $\Omega = 1.8$ for sine-wave forcing (Eqn. 25, initial condition ψ (λ,0)=0, and integrating to steady cycling conditions). The magnitude of the peak in average rate is 1.28 times the steady-state rate at the mean concentration on the high branch of the steady-state rate *vs.* concentration curve.

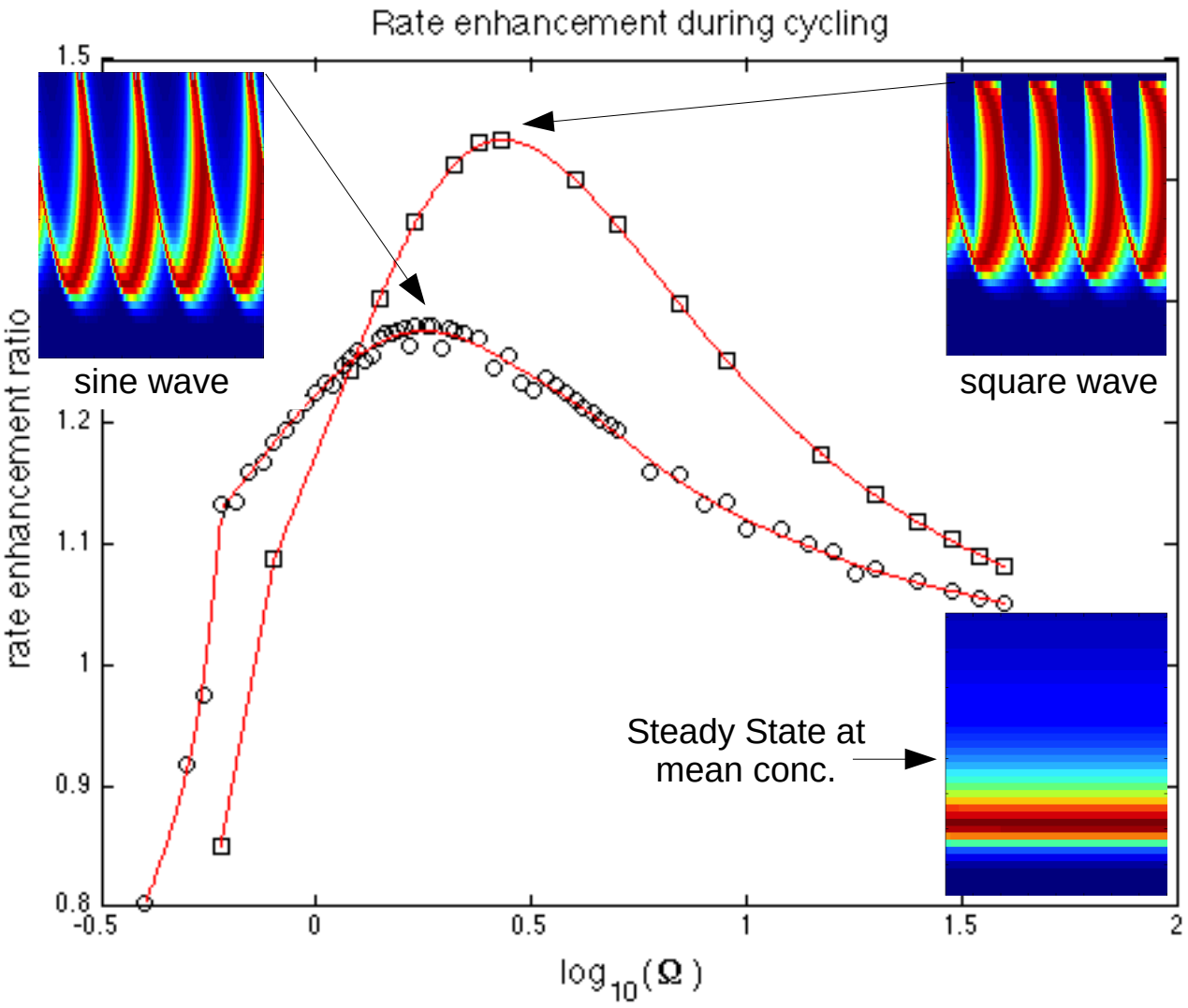

Fig. 3. Rate enhancement during reactant concentration forcing for the simplified kinetic model. The vertical axis is the ratio of the average reaction rate during cycling to the steady-state rate at the mean reactant concentration over the external boundary of the layer. The horizontal axis is the log of the dimensionless cycling frequency: $\log_{10}(\Omega)$. Circles: sine-wave forcing. Squares: square-wave forcing (on-off with 50% duty cycle). Color insets are space-time patterns of local reaction rate in the porous layer. $\kappa_{ads} = 100$ and $\phi = 34$.

As the forcing frequency increases above the peak frequency, the average rate during cycling approaches the steady-state rate at the mean concentration (on the high branch of the rate *vs.* concentration curve when rate multiplicities exist and when starting from an empty-surface initial condition). That is, the value of the rate enhancement ratio approaches one. At very high frequencies, the assumption of close approach to equilibrium adsorption in Eqn. 21 will not hold and detailed simulations using Eqn. 2 and Eqn. 8 can be used to extend the plot closer to the relaxed steady-state asymptote at high frequencies.

As the forcing frequency decreases below the peak frequency for these kinetics and parameter values ($\kappa_{ads} = 100$ and $\phi = 34$), the entire layer will go into the inhibited state (low branch of the rate *vs.* concentration curve) for part of the cycle, thus, causing the average rate during cycling to be less than the steady-state rate at the mean concentration on the high branch of the rate curve (rate enhancement ratio < 1). The onset of this condition at low frequency can be seen in Fig. 3 where the curve for sine-wave cycling has an abrupt change in slope at $\log_{10}(\Omega)$ = -0.22, $\Omega = 0.60$.

As discussed below, the peak rate occurs at $\Omega = 2.7$ for square-wave cycling *vs.* $\Omega = 1.8$ for sine-waves. The result that the peak rate occurs at about $\Omega = 2$ can be explained in terms of the rate at which the surface inside the layer can be filled by adsorbed reactant in the presence of diffusion resistance.

Consider a limiting case in which adsorption is fast such that the outer fraction of the porous catalyst layer that is exposed to any amount of gas-phase reactant at any time is fully covered and the remaining portion of the layer is empty. After an empty layer is suddenly exposed to a fixed external concentration of reactant gas, the time required to completely fill the internal surface in the layer with adsorbed reactant is:[7,30]

$$t_{\text{fill}}(s) = \frac{1}{2}(\epsilon\alpha)\left(\frac{L^2}{D_e}\right) \tag{27}$$

Note that increasing surface-to-gas capacity ratio α increases the time required to fill the

surface in the layer.

Now, if we force the system with a frequency that is the inverse of this surface filling time,

$$\omega(s^{-1}) = \frac{1}{t_{\text{fill}}(s)} = \frac{2}{\epsilon\alpha}\left(\frac{D_e}{L^2}\right) \tag{28}$$

we get the dimensionless frequency near which the peaks in average rate *vs.* cycling frequency are obtained:

$$\Omega = (\epsilon\alpha)\left(\frac{L^2}{D_e}\right)\omega \tag{29}$$

$$\Omega = 2 \tag{30}$$

This is an approximation, of course. The surface in the layer doesn't fill completely with adsorbed reactant, and a portion of the cycle period is needed to desorb and react adsorbed reactant. But this approximation does give a physical reason for the location of the peak. For the porous layer in Fig. 1, the peak in rate is at $\Omega = 0.8$ for sine-wave forcing of a complex $CO+O_2$ oxidation mechanism over a surface with two adsorbed reactants and two types of sites with different parameter values.

The presence and magnitude of a peak in rate *vs.* frequency is also related to the Thiele modulus ϕ and the adsorption equilibrium constant κ_{ads}. As the Thiele modulus decreases and adsorption constant increases, the potential for rate enhancement during periodic operation increases. Identification of the ranges of parameter values for which rate enhancement is possible is outside the scope of this work.

Eqn. 21 for the limiting condition was obtained for $\kappa_{rxn} << 1$ and $\alpha >> 1$. This is a single partial differential equation. For larger values of κ_{ads} and smaller values of α, solution of a stiff system of coupled differential equations may be required. The effect of such changes in the parameters will be to make the kinetics more linear and decrease the surface storage capacity, thus, lowering the rate enhancement during periodic operation.

Forcing Function Shape

Rate *vs.* frequency curves vary with the shape of the forcing function, as shown in Fig. 3. For these parameter values ($\kappa_{ads} = 100$ and $\phi = 34$), the peak in average rate during sine-wave cycling occurs at $\Omega = 1.8$ with a peak in average rate 1.28 times the steady-state rate at the mean concentration.

For the same conditions but with 50% duty-cycle, on-off square-wave forcing, the peak in rate occurs at $\Omega = 2.7$ with a peak in average rate 1.43 times the steady-state rate at the mean concentration.

Reaction over a porous catalyst tends to lessen the effects of changes in the shape of the forcing function relative to reaction over a hypothetical "flat" surface in the absence of mass transfer resistance.

Over the "flat" surface with no diffusion resistance, maximum rate enhancement can be obtained with on-off square-wave forcing in which the reactant is "on" for only a small fraction of the cycle. For these kinetics, the enhancement in average rate during cycling increases with an increase in κ_{ads}, i.e., for $k_1 >> k_{-1}$. This is because a relatively large amount of reactant is "stored" by adsorption over the surface during the "on" fraction of the cycle, when κ_{ads} is large and equilibrium coverage θ is high, for later reaction (plus desorption) during the "off" fraction of the cycle. Since the adsorption rate constant k_1 is relatively large, the surface fills to capacity in a relatively short period of time, i.e., short fraction of the cycle.

In contrast, over a porous catalyst layer, the filling and emptying of the surface throughout the layer is controlled by the dynamic diffusion coefficient and not k_1 and k_{-1}.

Conclusion

This work has discussed the importance of studying and, in some cases, operating porous heterogeneous catalysts under dynamic conditions. Focus was placed on the effects of internal diffusion resistance and the development of dimensionless scaling parameters for dynamic operation. Scott Fogler is to be complimented for including many sections in his textbooks

about dynamic operation of chemical reactors.

References

(1) Fogler, H. S. *Elements of Chemical Reaction Engineering, 4th ed.*; Prentice-Hall: New York, 2005.

(2) Fogler, H. S. *Essentials of Chemical Reaction Engineering*; Prentice-Hall: New York, 2010.

(3) Herz, R. K. *Reactor Lab*; educational software available at http://ReactorLab.net (accessed Sept. 29, 2014).

(4) Herz, R. K. Dynamic behavior of automotive three-way emission control systems, in *Catalysis and Automotive Pollution Control*; Elsevier: Amsterdam, 1987; pp. 427-444.

(5) Herz, R. K.; Marin, S. P. Surface chemistry models of carbon monoxide oxidation on supported platinum catalysts. *J. Catal.* **1980**, *65*, 281-296.

(6) Cho, B. K. Dynamic behavior of a single catalyst pellet 1. Symmetric concentration cycling during carbon monoxide oxidation over platinum/alumina. *Ind. Eng. Chem. Fundamen.* **1983**, *22*, 410-420.

(7) Racine, B. N.; Herz, R. K. Modeling dynamic CO oxidation over Pt/Al_2O_3: Effects of intrapellet diffusion and site heterogeneity. *J. Catalysis* **1992**, *137*, 158-178.

(8) Cannestra, A. F.; Nett, L. C.; Herz, R. K. Measurement of gas composition at the center of a porous pellet during adsorption and catalytic reaction under dynamic conditions. *J. Catalysis* **1997**, *172*, 346-354.

(9) Nett-Carrington, L. C.; Herz, R. K. Spatiotemporal patterns within a porous catalyst: dynamic carbon monoxide oxidation in a single-pellet reactor. *Chem. Eng. Sci.* **2002**, *57*, 1459-1474.

(10) Herz, R.K. Spatiotemporal patterns in a porous catalyst during light-off and quenching of carbon monoxide oxidation. *Chem. Eng. Sci.* **2004** *59*, 3983-3991.

(11) Silveston, P. L. *Composition modulation of catalytic reactors*; CRC Press, 1998.

(12) Silveston, P. L.; Hudgins, R. R. *Periodic Operation of Reactors*; Oxford : Elsevier

Science, 2012.

(13) Schädlich, K.; Hoffmann, U.; Hofmann, H. Periodical Operation of Chemical Processes and Evaluation of Conversion Improvements. *Chem. Eng. Sci.* **1983** *38*, 1375-1384.

(14) Silveston, P.; Hudgins, R.R.; Renken, A., 1995. Periodic operation of catalytic reactors-introduction and overview. *Catalysis Today* **1995** *25*, 91-112.

(15) Gutsche, R.; Lange, R.; Witt, W. The effect of process nonlinearities on the performance of a periodically operated isothermal catalytic reactor. *Chem. Eng. Sci.* **2003** *58*, 5055-5068.

(16) Alvarez, J.; Meraz, M.; Valdes-Parada, F.J.; Alvarez-Ramirez, J. First-harmonic balance analysis for fast evaluation of periodic operation of chemical processes. *Chem. Eng. Sci.* **2012** *74*, 256-265.

(17) Petkovska, M.; Nikolic, D.; Markovic, A., Seidel-Morgenstern, A. Fast evaluation of periodic operation of a heterogeneous reactor based on nonlinear frequency response analysis. *Chem. Eng. Sci.* **2010** *65*, 3632-3637.

(18) Paunic, D.N.; Perkovska, M. Evaluation of periodic processes with two modulated inputs based on nonlinear frequency response analysis. Case study: CSTR with modulatoin of the inlet concentration and flow-rate. *Chem. Eng. Sci.* **2013** *104*, 208-219.

(19) Hoebink, J.H.B.J.; Nievergeld, A.J.L.; Marin, G.B. CO oxidation in a fixed bed reactor with high frequency cycling of the feed. *Chem. Eng. Sci.* **1999** *54*, 4459-4468.

(20) Kočí, P.; Kubíček, M.; Marek, M. Periodic forcing of three-way catalyst with diffusion in the washcoat. *Catalysis Today* **2004** *98*, 345-355.

(21) Lee, C. K.; Bailey, J. E. Diffusion waves and selectivity modifications in cyclic operation of a porous catalyst, *Chem. Eng. Sci.* **1974**, *29*, 1157-1163.

(22) Crank, J.; Nicolson, P. A practical method for numerical evaluation of solutions of partial differential equations of the heat-conduction type. *Proceedings of the Cambridge Philosophical Society, Mathematical and Physical Sciences* **1947**, *43*, 50-67.

(23) Wei, J.; Becker, E. R. The optimum distribution of catalytic material on support layers

in automotive catalysis, in *ACS Adv. Chem. Ser. 143*; Amer. Chem. Soc.: Washington, DC, 1975;. Chapter 10, pp. 116-132.

(24) Harold, M. P.; Garske, M. E. Kinetics and multiple rate states of CO oxidation on Pt I. Model development and multiplicity analysis. *J. Catalysis* **1991**, *127*, 524-552.

(25) Eigenberger, G., Kinetic instabilities in heterogeneously catalyzed reactionsI: Rate multiplicity with langmuir-type kinetics. *Chem. Eng. Sci.* **1978** *33*, 1255-1261.

(26) Do, D.D.; Weiland, R.H. Substrate-inhibited kinetics with catalyst deactivation in an isothermal CSTR. II. Multiple pseudosteady states and reactor failure. *AIChE J.* **1980** *26*, 1020-1028.

(27) Racine, B.N.; Sally, M.J.; Wade, B.; Herz, R.K. Dynamic CO oxidation over Pt/Al2O3. *J. Catalysis* **1991** *127*, 307-331.

(28) Hsiao, H.-W. *Numerical Study of Reaction in Porous Catalysts under Composition Modulation*, Ph.D. dissertation, U. California, San Diego, 2010.

(29) Renken, A.; Hudgins, R. R.; Silveston, P. L. Use of Modulation in Mechanistic Studies, in *Periodic Operation of Reactors*, P. L. Silveston and R. R. Hudgins, eds.; Elsevier Science: Oxford, 2012; Chap. 13, pp. 369-386.

(30) Herz, R. K.; Shinouskis, E. J. Transient oxidation and reduction of alumina-supported platinum *Appl. Surf. Sci.* **1984** *19*, 373

Figure Captions

Fig. 1. Predicted patterns of local CO oxidation rate during sine-wave cycling of CO in constant O_2 over Pt/Al_2O_3. Curves are average overall rate during cycling vs. $\log_{10}$ of frequency. Black (peak on right) = hypothetical "flat" surface with no diffusion resistance. Blue (peak on left) = rate over 25 micron porous catalyst layer. Color insets are space-time patterns of local reaction rate in the porous layer. The model of Nett-Carrington and Herz[9] and the parameter values in Table 1 of that work apply for the porous layer, except that $\phi_1 = 0.20$ (fraction site-type 1) and $C^{surf}{}_{tot}$= 44 mol of total surface sites per m^3 layer. T = 140 °C, 0-16 Pa-CO, 110 Pa-O_2. Rate shown is turnover frequency (product molecules formed per site per second).

Fig. 2. Predicted steady-state CO oxidation rate vs. external CO pressure in constant O_2 over Pt/Al_2O_3. Dashed line = rate over hypothetical "flat" surface with no diffusion resistance. Double solid lines = rate over porous catalyst layer showing rate multiplicity. Same conditions as Fig. 1

Fig. 3. Rate enhancement during reactant concentration forcing for the simplified kinetic model. The vertical axis is the ratio of the average reaction rate during cycling to the steady-state rate at the mean reactant concentration over the external boundary of the layer. The horizontal axis is the log of the dimensionless cycling frequency: $\log_{10}(\Omega)$. Circles: sine-wave forcing. Squares: square-wave forcing (on-off with 50% duty cycle). Color insets are space-time patterns of local reaction rate in the porous layer. $\kappa_{ads} = 100$ and $\phi = 34$.